Nanoscale

ROYAL SOCIETY OF CHEMISTRY

PAPER

View Article Online
View Journal | View Issue

Cite this: *Nanoscale*, 2025, **17**, 5106

Boosting Cu ion capture in high-salinity environments with amino-functionalized millispheres†

Jiaming Hu,[a] Jianheng Hong,[a] Weiting Yu,[b] Xiuzhen Wei[a] and Meilan Pan*[a]

High salinity in wastewater often hampers the performance of traditional adsorbents by disrupting electrostatic interactions and ion exchange processes, limiting their efficiency. This study addresses these challenges by investigating the salt-promoted adsorption of Cu ions onto amino-functionalized chloromethylated polystyrene (EDA@CMPS) millispheres. The adsorbent was synthesized by grafting ethylenediamine (EDA) onto CMPS, which significantly improved Cu adsorption, achieving nearly three times the capacity in saline solutions (1.65 mmol g^{-1}) compared to non-saline solutions (0.66 mmol g^{-1}). Mechanistic analysis showed that the presence of salts, such as NaCl, promoted the protonation of amino groups on EDA@CMPS, increasing their positive charge and enhancing their affinity for Cu ions. The solution's ionic strength further amplified this protonation, reducing electrostatic repulsion between the adsorbent and the Cu ions, thus improving binding efficiency. Additionally, the increased ionic strength altered Cu speciation, favoring the formation of $Cu(NH_3)_4^{2+}$ complexes, which were more easily adsorbed. These synergistic effects resulted in faster adsorption kinetics, higher capacity, and improved Cu ion removal, particularly in saline environments. Overall, these findings bridge the gap between material design and functional performance in high-salinity wastewater, offering a promising strategy for efficient heavy metal removal and environmental remediation.

Received 30th October 2024,
Accepted 23rd December 2024

DOI: 10.1039/d4nr04517c

rsc.li/nanoscale

1. Introduction

The generation of heavy metal wastewater with variable salinity levels (*e.g.*, NaCl, Na_2SO_4, and $CaCl_2$) is common in several industries, including aquaculture in coastal areas, nuclear energy, and leather manufacturing.[1–3] These effluents often contain heavy metals with carcinogenic and toxic properties that are non-degradable and accumulate in organisms through the food chain, posing serious environmental and health risks. Among remediation methods, adsorption stands out as one of the most promising techniques due to its simplicity, cost-effectiveness, and potential for adsorbent recycling.[4–8] However, high salinity in wastewater poses a critical challenge: inorganic salts compete for adsorption sites, disrupt electrostatic interactions, and inhibit ion exchange processes, severely limiting the efficiency of conventional adsorbents.[9–11] Thus, developing high-performance adsorbents capable of maintaining their adsorption efficiency in high-salinity environments is critical for overcoming the limitations posed by salts in heavy metal wastewater treatment.

A variety of specialized functional adsorbents have been developed for treating heavy metal wastewater, including activated carbons derived from various sources, biomass-based materials, and synthetic polymers.[12–14] Among these, cross-linked polymer millispheres, with their uniform pore structure, extensive surface area, and tunable functional groups, have demonstrated potential as high-performance adsorbents.[15] However, their performance in saline wastewater remains underexplored. Specifically, competition between salt ions can diminish adsorption capacities, and current functionalization strategies often do not adequately mitigate these effects.[16] For example, sulfonic and carboxylic groups are effective in ion exchange but are easily disrupted by high salt concentrations, leading to reduced efficacy.[17–20] These limitations underscore the need for adsorbents that are not only resistant to salt interference, but also capable of leveraging saline environments to enhance adsorption.

Amine-functionalized materials have emerged as a promising solution for metal adsorption in challenging environments, including saline wastewater. The electron-donating properties of amine groups ($-NH_2$) enable strong chelation with

[a]*College of Environment, Zhejiang University of Technology, Hangzhou, Zhejiang 310014, China. E-mail: mlpan@zjut.edu.cn*
[b]*Shaoxing Research Institute, Zhejiang University of Technology, Shaoxing 312085, China*

†Electronic supplementary information (ESI) available: BJH specific surface areas, average pore diameters, pore volumes, and pore size distributions of EDA@CMPS and CMPS, N_2 adsorption–desorption isotherm curves, XPS spectra, kinetic parameters and intra-particle diffusion simulations for the adsorption of Cu^{2+} on EDA@CMPS in saline solution and non-saline solution, and zeta potentials of EDA + Cu in different salinities. See DOI: **https://doi.org/10.1039/d4nr04517c**

heavy metal ions, making them effective for adsorption applications.[21–23] However, under high-salinity conditions, the performance of these materials can vary significantly.[24,25] Inorganic salts can alter the protonation states of amine groups, which directly impacts their ability to bind metal ions. Some studies have shown that protonated amine groups ($-NH_3^+$) exhibit enhanced metal ion affinity, suggesting that the presence of salts could be leveraged to improve adsorption efficiency.[26] Nevertheless, achieving optimal functionality requires a balance between material design and the chemical dynamics induced by salinity.

This study aims to address these challenges by developing amino-functional chloromethylated polystyrene (EDA@CMPS) millispheres that exhibit superior adsorption capacity for Cu ions under saline conditions. By grafting ethylenediamine (EDA) onto CMPS, this material enhances the protonation of amino groups in the presence of salts, increasing their affinity for metal ions. This novel approach leverages the interactions between salt-induced protonation and Cu ion adsorption, achieving nearly three times the adsorption capacity in saline solutions compared to non-saline environments. Furthermore, this study provides detailed insights into the mechanisms underlying salt-promoted adsorption through experimental characterization and DLVO theory simulations. By bridging the gap between material design and functional performance in high-salinity wastewater, this work offers a promising strategy for efficient heavy metal removal and environmental remediation.

2. Experimental section

2.1. Chemicals and materials

Chloromethylated polystyrene (CMPS) millispheres were purchased from Zhengguang Co., Ltd (Hangzhou, China). The chemicals used in this study, including $Cu(NO_3)_2$, ethylenediamine (EDA), sodium sulfate (Na_2SO_4), sodium chloride (NaCl), calcium chloride ($CaCl_2$), sodium nitrate ($NaNO_3$), sodium phosphate (Na_3PO_4), magnesium chloride ($MgCl_2$), lead chloride ($PbCl_2$), potassium chloride (KCl), diethylamine (DEA), and trimethylamine (TMA), were all purchased from Sigma-Aldrich and used without further purification. The solutions were prepared using ultrapure water (18.25 MΩ cm) obtained from a Milli-Q system.

2.2. Preparation of EDA@CMPS

The EDA@CMPS millispheres were synthesized *via* two steps, including the swelling of CMPS and modification with EDA through a solvothermal reaction. Specifically, (1) swelling of CMPS: CMPS millispheres (D = 0.6–0.9 mm) were swollen in dichloromethane for 12 h (25 °C). This swelling process is essential for enhancing the accessibility of the polymer's surface for the grafting reagents and increasing the efficiency of subsequent functionalization. (2) Grafting of EDA: after swelling, the CMPS millispheres were treated with EDA in ethanol solution for 24 h at 80 °C. The solvent choice was based on the ability of ethanol to dissolve EDA and ensure a homogeneous reaction environment while also facilitating the nucleophilic substitution of chloromethyl groups ($-CH_2Cl$) on the CMPS surface with EDA. (3) Post-grafting processing: following the grafting reaction, the modified millispheres (EDA@CMPS) were subjected to Soxhlet extraction with ethanol to remove untreated EDA and any residual solvents. The extraction step ensures that only the functionalized material remains free from any excess reactants that could interfere with subsequent adsorption experiments. Finally, the EDA@CMPS millispheres were dried at 50 °C for 12 hours to remove any residual solvent, ensuring a clean and stable final product.

2.3. Characterization

The microscopic features, morphology and element distribution were characterized using scanning electron microscopy with energy dispersive spectroscopy (SEM-EDS, Bruker Nano, Berlin, Germany). Brunauer–Emmett–Teller (BET) measurements using N_2 adsorption were performed using an Autosorb-IQ-MP (Quantachrome) surface area analyzer. The surface functional groups were characterized using Fourier transform infrared spectroscopy (FT-IR, Nicolet 6700, Thermo, USA) and X-ray photoelectron spectroscopy (XPS, Thermo 250Xi, USA). Zeta potential analysis was performed using a zeta potential analyzer (Malvern, Nano ZS90). The surface properties were characterized using contact angle measurement (Dataphysics, OCA50AF, Germany).

2.4. Adsorption experiments

The traditional bottle-point method was used to evaluate the adsorption performance. The adsorption experiments for Cu ions were carried out by dispersing 0.05 g of adsorbents in 50 ml of predetermined concentrations of cupric nitrate (0.5 mM) with varying amounts (5–50 mM) of salts (NaCl, $NaNO_3$, $Ca(NO_3)_2$, Na_2SO_4, NaH_2PO_4, KNO_3, $Mg(NO_3)_2$, $Pb(NO_3)_2$, and $Mg(NO_3)_2$) to provide salinity. The mixture was then stirred for 24 h to ensure adsorption equilibrium. The concentration of Cu ions was determined using an atomic adsorption spectrophotometer (AAS, Persee, TAS-990F).

Meilan Pan

Dr Meilan Pan recevied her Ph. D. in Environmental Science and Engineering from Nankai University, China, in 2018. She then joined the School of Chemical and Biomedical Engineering at Nanyang Technological University, Singapore, as a research fellow. Currently, She is a full professor in the College of Environment at Zhejiang University of Technology in Hangzhou, China. Her research focuses on the design of highly efficient functional catalysts and their applications in environmental remediation.

The adsorption capacity of Cu ions on the adsorbents can be calculated using the following eqn (1):

$$Q_m = \frac{(C_o - C_e)V}{m} \quad (1)$$

where Q_m (mmol g^{-1}) is the equilibrium adsorption capacity of the Cu ions on the adsorbent, C_o and C_e (mmol L^{-1}) are the initial and equilibrium concentrations of Cu ions, V (L) is the volume of the pollutant solution, and m (g) is the mass of the adsorbent.

3. Results and discussion

3.1 Characterization of the adsorbents

The EDA@CMPS adsorbent was synthesized by uniformly grafting ethylenediamine (EDA) onto chloromethylated polystyrene (CMPS) spheres *via* a substitution reaction, yielding NH_2-functionalized surfaces (Fig. 1a). Elemental mapping showed a uniform distribution of nitrogen throughout the sphere (Fig. 1b and c), while the intrinsic pore structure of CMPS was retained following the grafting process (Fig. 1d). The introduction of $-NH_2$ groups increased the surface hydrophilicity, reducing the contact angle from 82° to 61°. As shown in Table S1 and Fig. S1,† the specific surface area, pore volume, and average pore size of EDA@CMPS millispheres increased slightly post-grafting, indicating that additional crosslinking partially blocked some pores while generating new surface areas (Fig. 1e). FTIR and XPS analyses confirmed the successful chemical modification of EDA@CMPS (Fig. 1f and g). Specifically, the disappearance of the peaks of the benzenoid chloromethyl group ($-CH_2Cl$) at 678.8 and 1268.9 cm^{-1}, along with a blue shift in the O–H bond peak from 3424 cm^{-1} to 3403 cm^{-1}, confirmed the substitution of $-CH_2Cl$ groups

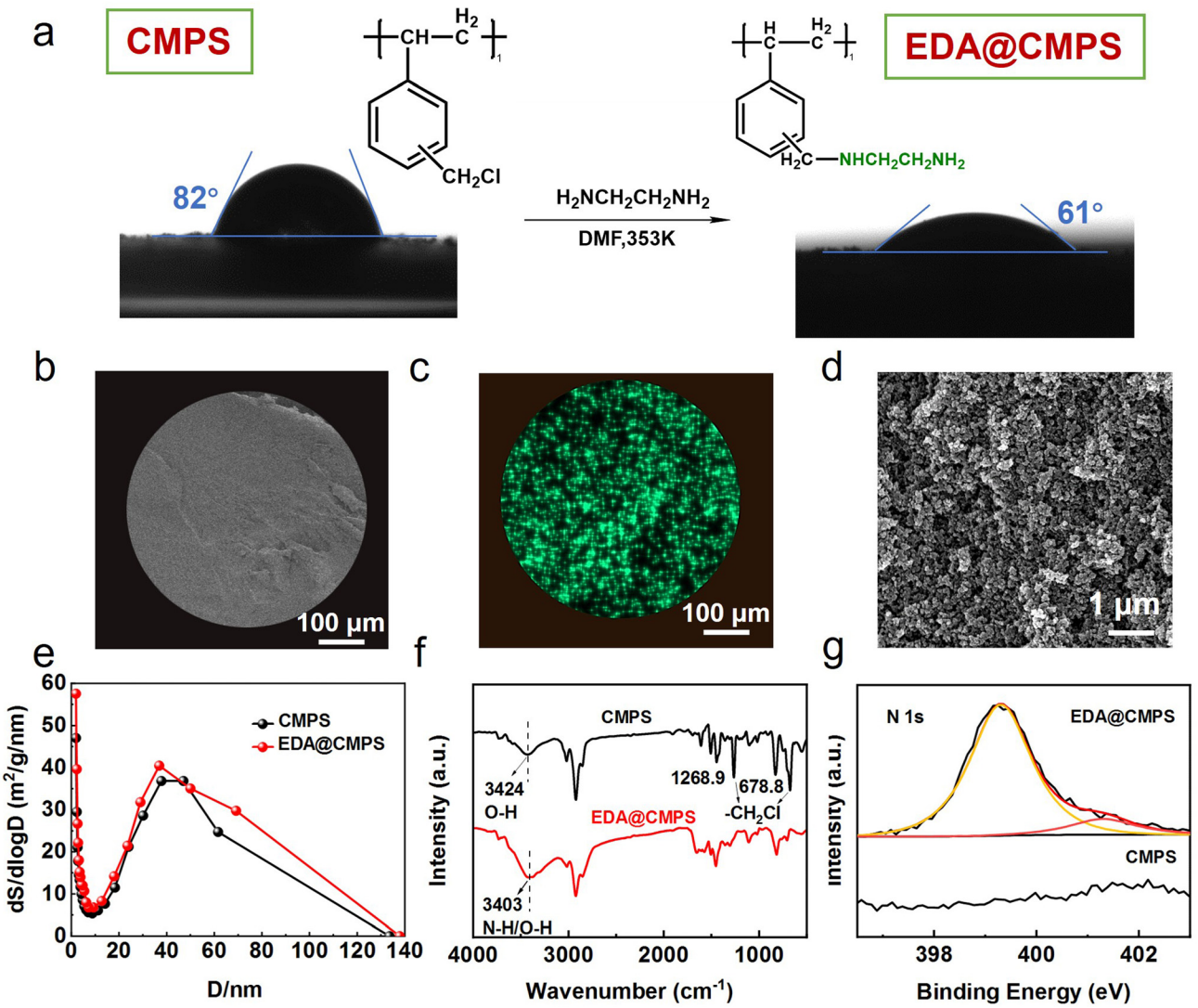

Fig. 1 (a) Schematic illustration of EDA@CMPS fabrication. Photograph (b), EDS mapping (c) and SEM image (d) of EDA@CMPS. Pore size distribution in BET analysis (e), FTIR spectra (f), and N 1s spectra in XPS analysis (g) of CMPS and EDA@CMPS.

with EDA. Additionally, the overlap of N–H bonds with O–H bonds further confirmed the presence of $-NH_2$ groups. In the N 1s XPS spectrum, peaks corresponding to amine groups (N–H) at 399.2 eV and their protonated form ($-N^+$) at 400.5 eV validated the successful EDA grafting and protonation on the CMPS surface.

3.2 Adsorption capacity of functional adsorbents in saline environments

Fig. 2a illustrates the effects of various salts and their concentration on the adsorption of Cu ions by several functionalized millispheres in saline wastewater. Four types of functionalized millispheres were tested: EDA@CMPS (amine functionalized), SA@CMPS (sulfuric acid functionalized), TA@CMPS (trimethylamine functionalized), and DA@CMPS (dimethylamine functionalized). The adsorbents were exposed to Cu solution containing either NaCl or $Ca(NO_3)_2$ salts, with varying concentrations of each salt (Fig. 2b and c). As the concentration of NaCl increased, the adsorption capacity of Cu ions onto EDA@CMPS increased significantly, from 0.66 to 1.65 mmol g^{-1} at 50 mM NaCl, which is consistent with the results observed for $Ca(NO_3)_2$ (from 0.66 to 1.60 mmol g^{-1}). Interestingly, the adsorption capacity of DA@CMPS in the absence of salts was negligible, but when exposed to 50 mM NaCl (1.70 mmol g^{-1}) or $Ca(NO_3)_2$ (1.67 mmol g^{-1}), its adsorption performance was notably enhanced. In contrast, the adsorption capacity of SA@CMPS decreased with increasing NaCl concentration, dropping from 1.90 mmol g^{-1} to 0.57 mmol g^{-1} at 50 mM NaCl, and was completely inhibited by the presence of $Ca(NO_3)_2$, decreasing to 0 mmol g^{-1}. These findings suggest that the functionalization of CMPS with EDA and DA introduces more active sites, significantly improving their adsorption of Cu ions under saline conditions. In contrast, functionalization with TA and SA did not provide similar benefits. Therefore, the results demonstrate that the grafting of functional amine groups onto CMPS enhances its affinity for Cu ions, particularly in saline environments where the ionic strength reduces electrostatic repulsion and promotes stronger binding. These findings underscore the effectiveness of grafting functional groups to improve the adsorbent's performance under high-salinity conditions, as evidenced by a substantial increase in adsorption capacity compared to non-salinity solutions.

3.3 Salt-promoting adsorption efficiency of EDA@CMPS

The $-NH_2$ groups of EDA on EDA@CMPS serve as the primary adsorption sites for Cu ions, as evidenced by the shift in the N 1s binding energy from 399.29 eV to 399.11 eV following Cu adsorption (Fig. S2†). Furthermore, the Cu adsorption performance of EDA@CMPS improved with increasing salt concentration (Fig. 3a–c), with the detailed adsorption capacity quantified using atomic absorption spectroscopy (AAS). The results demonstrated that the adsorption capacity of EDA@CMPS increased approximately threefold upon the addition of 50 mM NaCl (0.66 mmol g^{-1} in the absence of NaCl *versus* 1.65 mmol g^{-1} in NaCl solution), confirming the enhancing effect of salts on the $-NH_2$ groups as adsorption sites for Cu ions. Fig. 3d illustrates the equilibrium adsorption capacity of EDA@CMPS as a function of the equilibrium Cu concentration (Ce). The results indicate that

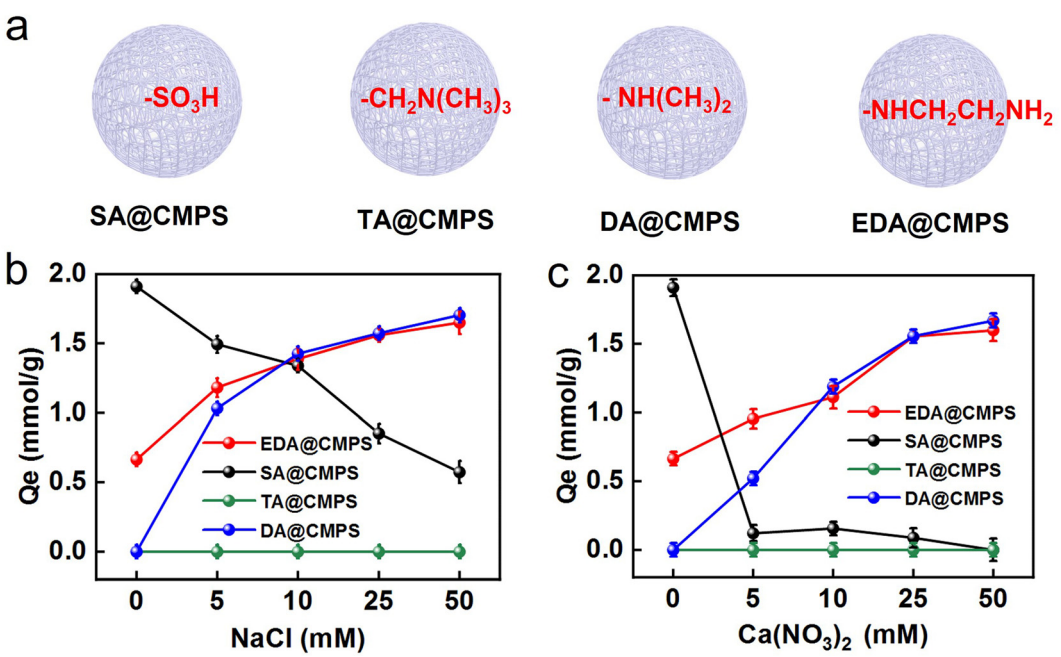

Fig. 2 (a) Schematic illustration showing several functional millispheres (EDA@CMPS, SA@CMPS, TA@CMPS, and DA@CMPS). Adsorption capacities of different functional CMPS millispheres at different concentrations of NaCl (b) and $Ca(NO_3)_2$ (c) solutions. [EDA@CMPS] = 1 g L^{-1}; [Cu^{2+}] = 0.5 mM; [NaCl] = 5–50 mM; [$Ca(NO_3)_2$] = 5–50 mM.

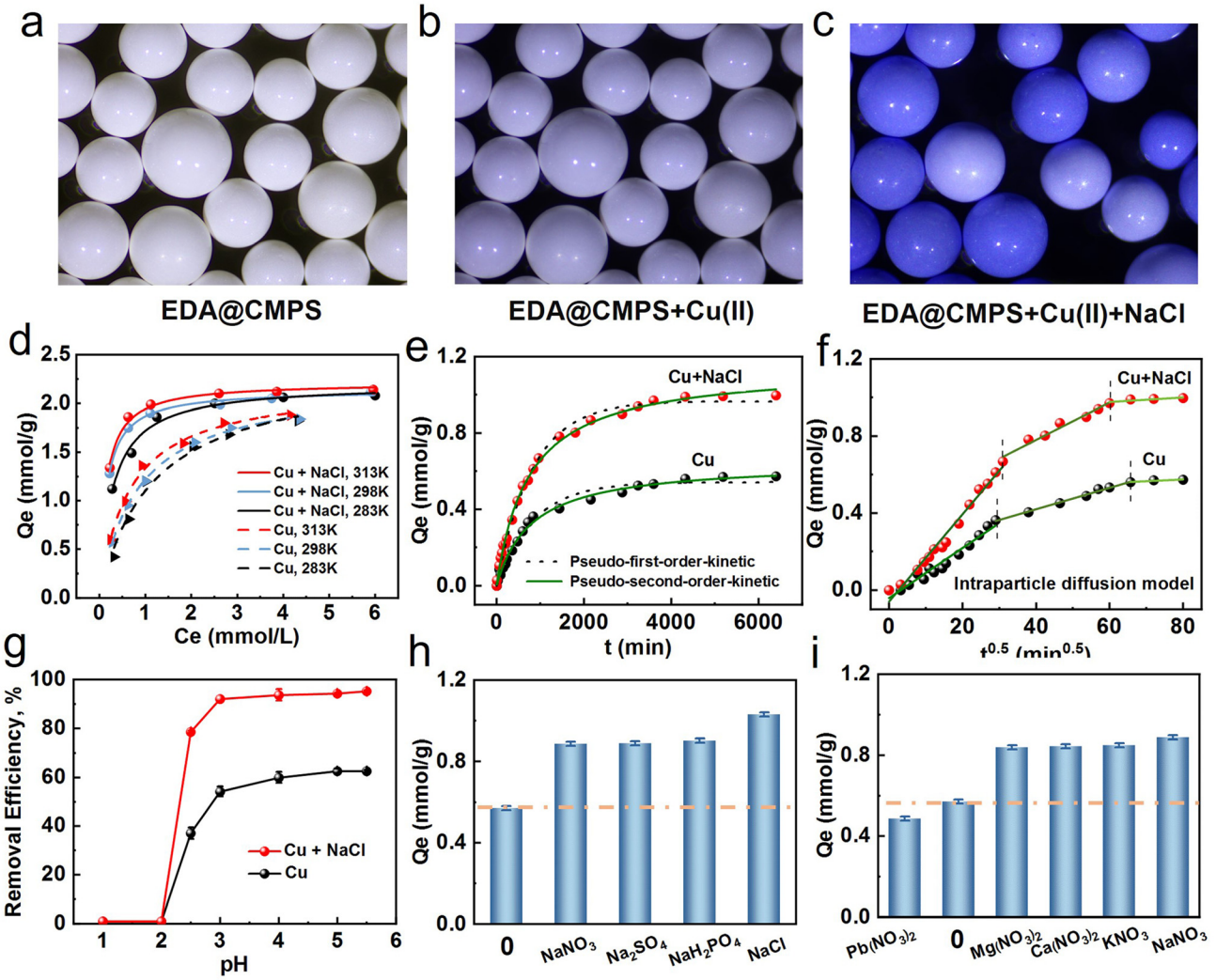

Fig. 3 (a) Photograph of EDA@CMPS before adsorption of Cu ions. (b) Photograph of EDA@CMPS after adsorption of Cu ions in the absence of NaCl. (c) Photograph of EDA@CMPS after the adsorption of Cu ions in the presence of NaCl. (d) Adsorption isotherms of Cu onto EDA@CMPS at varying temperatures (283 K, 298 K, and 313 K) and in the presence of NaCl. (e) Adsorption kinetics of Cu on EDA@CMPS in both Cu alone and Cu + NaCl solution analyzed using pseudo-first-order and pseudo-second-order models. (f) Interparticle diffusion model applied to Cu adsorption kinetics in the presence and absence of NaCl. [EDA@CMPS] = 0.4 g L^{-1}; [NaCl] = 5 mM; [Cu^{2+}] = 0.5 mM; T = 25 °C. (g) Dependence of pH on EDA@CMPS in Cu and Cu + NaCl. Effect of competing anions (h) and cations (i) on the adsorption efficiency of EDA@CMPS. [$NaNO_3$], [Na_2SO_4], [NaH_2PO_4], [NaCl], [$Pb(NO_3)_2$], [$Mg(NO_3)_2$], [$Ca(NO_3)_2$], and [KNO_3] were 5 mM.

the adsorption capacity increases with temperature in both single and competitive systems, suggesting the endothermic nature of the adsorption process. Notably, the adsorption capacity rises steadily with increasing equilibrium Cu concentration, reaching a maximum value of 2.14 mmol g^{-1}, beyond which it remains nearly constant. The presence of NaCl significantly accelerated the attainment of the maximum adsorption capacity. To analyze the salt-induced enhancement of Cu adsorption and examine the adsorption kinetics, both the pseudo-first-order and pseudo-second-order models were applied. The linearized pseudo-first-order kinetic model is:[27]

$$\ln(C_0 - C_t) = \ln C_0 - k_1 t \quad (2)$$

The pseudo-second-order model is linearly demonstrated as given in (eqn 3):[28]

$$\frac{t}{q_t} = \frac{1}{k_2 q_e^2} + \frac{t}{q_e} \quad (3)$$

where q_e is the adsorption capacity at equilibrium of Cu (mmol g^{-1}), q_t is the adsorption capacity of Cu (mmol g^{-1}) at time t, k_1 is pseudo-first-order rate constant (min^{-1}) and k_2 is pseudo-second-order rate constant (min^{-1}).

Fig. 3e shows that the adsorption kinetics of Cu ions are best described by the pseudo-secondary-order model. The results indicate that the adsorption rate of Cu ions increased with the addition of NaCl, with rates of 2.7×10^{-2} min^{-1} in the Cu + NaCl solution compared to 1.3×10^{-2} min^{-1} in the Cu ion

solution alone, confirming the salt-promoting effect of NaCl on Cu adsorption by EDA@CMPS. Furthermore, the intra-particle diffusion model was applied to investigate the diffusion mechanisms and rate-limiting steps during different stages of adsorption (Fig. 3f). The intra-particle diffusion model is:[29]

$$q_t = k_{ip} t^{0.5} + C \quad (4)$$

where q_t are the adsorption capacities at equilibrium and at time t (mmol g^{-1}), k_{ip} (mg [g $min^{0.5}$]$^{-1}$) is the intra-particle diffusion rate constant, and C is the intercept relating to the thickness of the boundary layer (mmol g^{-1}).

As shown in Fig. 3f and Table S2,† the adsorption process consists of three stages: (1) a rapid surface adsorption stage; (2) an intraparticle diffusion adsorption stage; and (3) an equilibrium adsorption stage. It is evident that the adsorption rate in all three stages is higher in the presence of NaCl compared to the system without NaCl.

The effect of pH on the salt-promoted adsorption of Cu ions on EDA@CMPS is illustrated in Fig. 3g. At pH values below 3, Cu adsorption efficiency is low, decreasing to nearly zero when the pH value drops below 2. This is attributed to the protonation of amino groups at low pH (Fig. S3†), which passivates the adsorption sites, thereby suppressing metal adsorption. However, the adsorption efficiency increases at higher pH levels, and the salt-promoting effect of EDA@CMPS becomes more pronounced when the pH exceeds 2. Under neutral pH conditions, amino groups are favorable for metal complexation. Thus, we propose that the introduction of salts promotes the complexation of amino groups and metal ions. Fig. 3h and i demonstrate that the promotion of Cu adsorption is primarily dependent on the cations and anions present. Different anions ($NaNO_3$, Na_2SO_4, Na_2HPO_4, and NaCl) all promote adsorption. Among cations, except Pb^{2+}, which inhibits adsorption due to specific interaction with $-NH_2$ groups,[30] other cations (*e.g.* Mg^{2+}, Ca^{2+}, K^+, and Na^+) significantly enhance the Cu adsorption capacity.

3.4 Salt-promoting mechanism of EDA@CMPS

Based on the above results, salts (such as NaCl, $Ca(NO_3)_2$, *etc.*) promote Cu adsorption on amino-functionalized (primary, secondary, and tertiary amine) millispheres. Cu ions can exist in various species, and understanding the mechanism by which salts enhance adsorption is crucial. In the absence of external ligands, Cu ions undergo hydrolysis to form a series of species, including: (a) primary hydrolysis, leading to low-molecular-weight complexes such as $Cu(OH)^+$, $Cu_2(OH)_2^{2+}$, and $Cu_3(OH)_4^{2+}$ and (b) the precipitation of copper oxides and hydroxides (*e.g.*, amorphous $Cu(OH)_m$, CuO(OH), and CuO). The speciation of Cu ions under experimental conditions was analyzed using Visual MINTEQ (version 3.1, Fig. 4a),[31] and the modeled species included both dissolved and colloidal Cu, consistent with the pathways described above. In agreement with previous studies,[32] adding NaCl enhances the formation of colloid Cu, such as $Cu_3(OH)_4^{2+}$, and leads to the disappearance of dissolved Cu ions at an NaCl concentration of 5 M. As shown in Fig. 4b, the surface ζ potential of EDA@CMPS decreased significantly to −0.1 mV upon the addition of NaCl, compared with ~5.2 mV in the absence of salts, indicating efficient chemical adsorption on EDA@CMPS. Moreover, the pH in the presence of NaCl was notably lower than in its absence (Fig. 4c and d), suggesting an increase in the protonation degree due to the salt addition. The adsorption capacity was positively correlated with pH, indicating that the protonation degree of the adsorbent plays a crucial role in enhancing adsorption. Therefore, at high NaCl concentrations, most Cu ions exists as colloidal $Cu_3(OH)_4^{2+}$, while the protonation degree of EDA on EDA@CMPS is enhanced, synergistically improving its Cu adsorption performance.

3.5 Contribution of protonation

To further investigate the adsorption mechanism of EDA@CMPS for Cu ions, three representative compounds—ethylenediamine (EDA), diethylamine (DEA), and trimethylamine (TMA)—were examined. As previously mentioned, most Cu ions exist as colloidal $Cu_3(OH)_4^{2+}$, which facilitates its complex adsorption onto the absorbents. A distinct Tyndall effect, while a purple solution formed in the Cu/DEA mixture, confirms the formation of Cu complexes (Fig. 5a–c). Additionally, the UV-vis spectra (Fig. 5d–f) further support the complexation between Cu ions and EDA, DEA, or TMA, as evidenced by the appearance of characteristic peaks corresponding to Cu complexes.

The interaction between the Cu ions and the amino groups led to the compression of the electronic double layers, resulting in a decrease in ζ potential (Fig. 5g–i). Notably, the change in potential with increasing EDA concentration was negligible, unlike the significant changes observed with DEA and TMA. This suggests a stronger colloidal interaction between the Cu ions and DEA/TMA compared to EDA.

pH is a critical parameter that influences both the conversion of colloidal Cu species and the surface properties, including the protonation degree of functional groups on the adsorbent. In the presence of NaCl, the pH rapidly decreased to approximately 6.82 from an initial value of 5.5, while the equilibrium pH was around 6.63 in the absence of NaCl. This trend is consistent across different initial pH values. At pH = 5.5, EDA@CMPS exhibited a positive charge, and its adsorption capacity was highly pH-dependent, indicating that electrostatic interactions and ion exchange are key factors in Cu adsorption.[33] Herein, $-NH_3^+$ and Cu ions were taken as representatives, and the adsorption mechanisms could be explained as follows (eqn (5)–(7)):

$$\text{CMPS-NH}_2 + H^+ \rightarrow \text{CMPS-NH}_3^+ \quad (5)$$

$$3Cu^{2+} + 4OH^- \rightarrow Cu_3(OH)_4^{2+} \quad (6)$$

$$\text{CMPS-NH}_3^+ + Cu_3(OH)_4^{2+} \rightarrow \text{CMPS-Cu}(NH_3)_4^{2+} \quad (7)$$

With the addition of NaCl, the adsorption of Cu ions was enhanced due to an increased protonation degree of the amino groups, which led to the consumption of H^+ and conse-

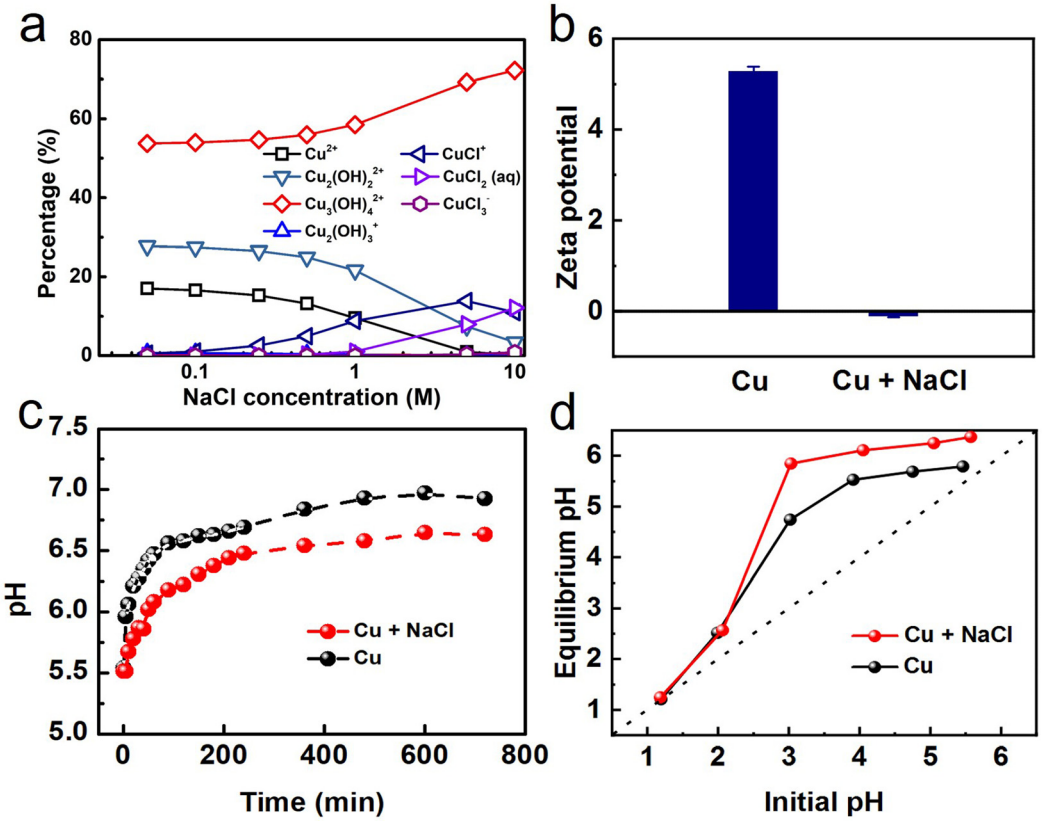

Fig. 4 (a) Speciation of Cu^{2+} ions in aqueous solution disordered by different concentrations of NaCl simulated by visual MINTEQ. (b) Effect of NaCl on the zeta potential of EDA@CMPS. (c) pH evolution with the adsorption of Cu ions. (d) Equilibrium pH *versus* initial pH. [Cu] = 32 mg L^{-1}; [NaCl] = 10 mM; [EDA@CMPS] = 1 g L^{-1}.

quently a higher equilibrium pH.[34,35] Furthermore, Cl^- can interact with the EDA@CMPS surface, likely due to the smaller hydration shells around the Cl^- ions. As Cl^- approaches the hydrated surface of EDA@CMPS, it incurs a lower energy penalty by removing or restructuring its hydration shell. This interaction neutralizes some of the negatively charged sites on the surface of EDA@CMPS, reducing the net negative charge. In other words, the repulsive forces between EDA@CMPS and Cl^- are diminished, while attractive forces become more dominant, thereby enhancing the adsorption capacity.

3.5 DLVO theory and its role in Cu adsorption

To understand how salts influence the adsorption of Cu ions on EDA@CMPS, we applied the Derjaguin–Landau–Verwey–Overbeek (DLVO) theory, which helps predict how particles interact in solution.[36–38] According to the DLVO theory (the detailed calculation methods are shown in the ESI†), the interaction between particles is governed by two opposing forces: attractive forces (such as van der Waals forces) and repulsive forces (mainly electrostatic repulsion). The balance between these forces determines how well particles, like EDA@CMPS, can absorb ions form a solution. Fig. 6a shows the interaction energy profiles for EDA@CMPS and Cu ions in a solution with a certain ionic strength. The interaction energy profiles, calculated using the known properties of EDA@CMPS (Table S3†), Cu ions, and water, reveal key insights about how salts affect the adsorption process. When NaCl is added to the solution, the zeta potentials of both EDA@CMPS and Cu ions decrease (Table S4†). The zeta potential is a measure of the surface charge on particles, and its reduction indicates that the electrostatic repulsion between particles is weakened. As a result, the height of the repulsive energy barrier (shown in the interaction energy profile) is reduced. Specifically, the predicted energy barrier drops from 79.1 kT at a low ionic strength (0.005 M NaCl) to 7.65 kT at higher ionic strength (0.5 M NaCl). This reduction in the energy barrier means that particles have a higher chance of overcoming repulsive forces and reaching the primary minimum, where adsorption occurs.

In addition to the primary minimum, the DLVO theory also predicts the formation of a secondary minimum in the interaction energy profile (Fig. 6b). At higher ionic strengths, the secondary minimum becomes deeper, meaning that the adsorption process becomes more favorable, even under less-than-ideal conditions. The deeper the secondary minimum, the easier it is for particles to settle in this energy state and be captured by the adsorbent. Salts reduce the strength of the repulsive forces between the adsorbent and the metal ions. The ions from the salt surround the particles, effectively "shielding" their charges and reducing the electrostatic repulsion. This allows the adsorbent to attract and bind with Cu

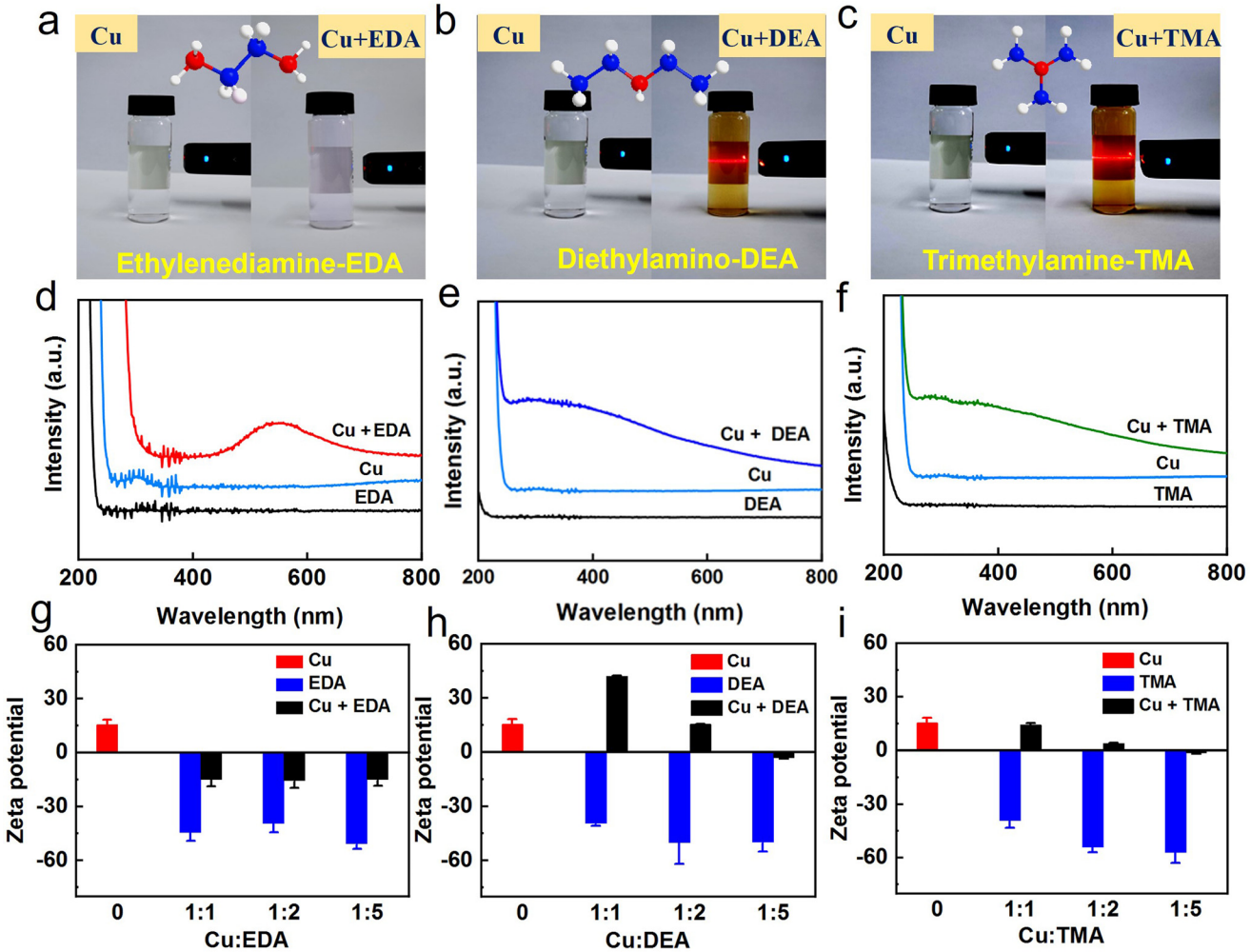

Fig. 5 Tyndall effects in EDA (a), DEA (b), and TMA (c) solutions. (d–f) UV-vis spectra of Cu, EDA/DEA/TMA, and Cu + EDA/DEA/TMA. (g–i) Zeta potentials of Cu and different amino compounds. [Cu] = 32 mg L^{-1}; [EDA] = 2.5 mM; [DEA] = 2.5 mM; [TMA] = 2.5 mM; [1 : 1] = 0.5 mM [Cu] : 0.5 mM [EDA]/[DEA]/[TMA]; [1 : 2] = 0.5 mM [Cu] : 1 mM [EDA]/[DEA]/[TMA]; [1 : 5] = 0.5 mM [Cu] : 2.5 mM [EDA]/[DEA]/[TMA].

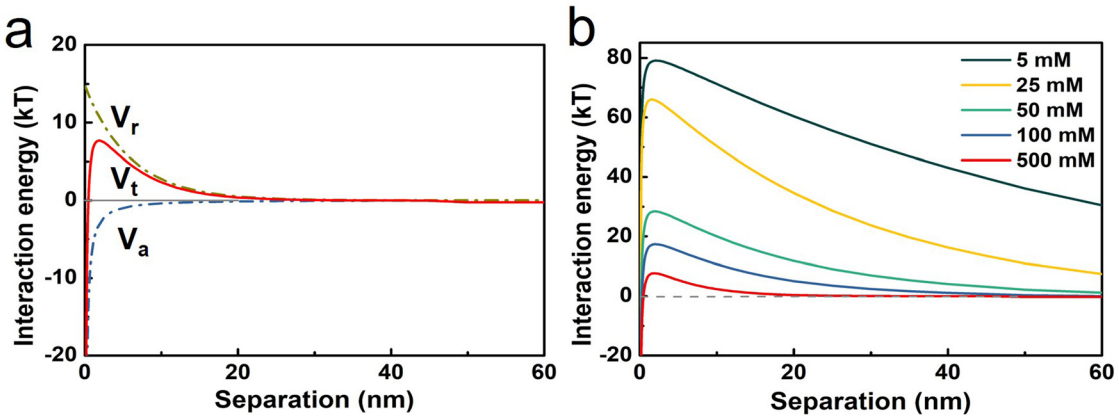

Fig. 6 (a) Interaction energy profile for EDA@CMPS–copper in 0.5 M NaCl. V_a, van der Waals forces, V_r, electric double layer forces, and V_t, total potential. (b) Interaction energy profile for EDA@CMPS–copper in 5, 25, 50, 100, and 500 mM NaCl *versus* the separation distance calculated by the DLVO theory.

ions more easily. As the salt concentration increases, the attractive forces dominate over the repulsive forces, enhancing the adsorption process. In simpler terms, higher salt concentrations make it easier for the absorbent to capture more Cu ions, which is crucial for improving its performance in high-salinity environments. Thus, the presence of salts like NaCl not only helps reduce repulsive forces, but also promotes the binding of Cu to EDA@CMPS, improving its efficiency in adsorbing metal ions from saline wastewater.

4. Conclusion

In summary, this study investigates the salt-promoted adsorption of heavy metal ions (Cu ions as representative ions) onto amino-functionalized millispheres (EDA@CMPS). The adsorbent was synthesized by grafting ethylenediamine (EDA) onto chloromethylated polystyrene (CMPS) millispheres, resulting in a material capable of achieving nearly three times the adsorption capacity for Cu ions in saline solutions (1.65 mmol g^{-1}) compared to non-saline solutions (0.66 mmol g^{-1}). Mechanistic analysis reveals that salts significantly enhance Cu ion adsorption on EDA@CMPS through the combined effects of protonation, ionic strength, and Cu speciation. The presence of salts, such as NaCl, promotes the protonation of amino groups on EDA@CMPS, increasing their positive charge and thereby enhancing their affinity for Cu ions. This protonation is further amplified by the ionic strength of the solution, which reduces electrostatic repulsion between the adsorbent and the Cu ions, thereby facilitating stronger binding. Additionally, increased ionic strength alters Cu speciation, favoring the formation of more easily adsorbed complexes, such as $Cu(NH_3)_4^{2+}$. These synergistic effects lead to higher adsorption capacity, faster kinetics, and improved Cu removal efficiency in saline environments, highlighting the importance of optimizing adsorbent materials for wastewater treatment under high-salinity conditions. This study provides new insights into the complex adsorption behavior of amino-functionalized CMPS in saline heavy metal wastewater.

Data availability

The data that support the findings of this study are available from the corresponding author upon reasonable request. Additional information can be found in the online ESI.†

Conflicts of interest

The authors declare no competing interests.

Acknowledgements

We gratefully acknowledge the Basic Scientific Research Projects in Colleges and Universities funded by Zhejiang Province (RF-A2022009) and the Shaoxing Science and Technology Plan Project (2024A11002).

References

1 J. Ju, Y. Feng, H. Li, X. Li and Q. Zhang, Recovery of valuable metals and NaCl from cobalt-rich crust and industrial waste salt via roasting coupling technology, *J. Sustain. Metall.*, 2021, 7(4), 1862–1875.
2 C. Z. Torma and E. Cséfalvay, Nanofiltration and electrodialysis: Alternatives in heavy metal containing high salinity process water treatment, *Chem. Pap.*, 2018, **72**(5), 1115–1124.
3 A. Azimi, A. Azari, M. Rezakazemi and M. Ansarpour, Removal of heavy metals from industrial wastewaters: A review, *ChemBioEng Rev.*, 2017, **4**(1), 37–59.
4 Z. Liu, L. Wang, Y. Lv, X. Xu, C. Zhu, F. Liu and A. Li, Impactful modulation of micro-structures of acid-resistant picolylamine-based chelate resins for efficient separation of heavy metal cations from strongly acidic media, *Chem. Eng. J.*, 2021, **420**, 129684.
5 E. Eskandari, M. Kosari, M. H. Davood Abadi Farahani, N. D. Khiavi, M. Saeedikhani, R. Katal and M. Zarinejad, A review on polyaniline-based materials applications in heavy metals removal and catalytic processes, *Sep. Purif. Technol.*, 2020, **231**, 115901.
6 G. Lofrano, M. Carotenuto, G. Libralato, R. F. Domingos, A. Markus, L. Dini, R. K. Gautam, D. Baldantoni, M. Rossi, S. K. Sharma, M. C. Chattopadhyaya, M. Giugni and S. Meric, Polymer functionalized nanocomposites for metals removal from water and wastewater: An overview, *Water Res.*, 2016, **92**, 22–37.
7 B. Pan, B. Pan, W. Zhang, L. Lv, Q. Zhang and S. Zheng, Development of polymeric and polymer-based hybrid adsorbents for pollutants removal from waters, *Chem. Eng. J.*, 2009, **151**(1–3), 19–29.
8 D. Chen, W. Shen, S. Wu, C. Chen, X. Luo and L. Guo, Ion exchange induced removal of Pb(II)by MOF-derived magnetic inorganic sorbents, *Nanoscale*, 2016, **8**, 7172.
9 Y. Liu, J. Wang, Y. Wang, H. Zhu, X. Xu, T. Liu and Y. Hu, High-flux robust PSf-b-PEG nanofiltration membrane for the precise separation of dyes and salts, *Chem. Eng. J.*, 2021, **405**, 127051.
10 J. Wang, W. Yu, N. J. D. Graham and L. Jiang, Evaluation of a novel polyamide-polyethylenimine nanofiltration membrane for wastewater treatment: Removal of Cu^{2+} ions, *Chem. Eng. J.*, 2020, **392**, 123769.
11 J. Church, J. H. Hwang, K. T. Kim, R. Mclean, Y. K. Oh, B. Nam, J. C. Joo and W. H. Lee, Effect of salt type and concentration on the growth and lipid content of *Chlorella vulgaris* in synthetic saline wastewater for biofuel production, *Biotechnol. Tech.*, 2017, **243**, 147–153.
12 D. Zhang and J. Li, Ordered SBA-15 mesoporous silica with high amino-functionalization for adsorption of heavy metal ions, *Chin. Sci. Bull.*, 2012, **58**(8), 879–883.

13 S. Wang, K. Wang, C. Dai, H. Shi and J. Li, Adsorption of Pb^{2+} on amino-functionalized core–shell magnetic mesoporous SBA-15 silica composite, *Chem. Eng. J.*, 2015, **262**, 897–903.
14 Y. Sun, F. Yu, L. Li and J. Ma, Adsorption–reduction synergistic effect for rapid removal of Cr(VI) ions on superelastic NH_2-graphene sponge, *Chem. Eng. J.*, 2021, **421**, 129933.
15 I. Kenawy, M. Hafez and R. Lashein, Thermal decomposition of chloromethylated poly (styrene)-PAN resin and its complexes with some transition metal ions, *J. Therm. Anal. Calorim.*, 2001, **65**(3), 723–736.
16 Y. Chen, B. Pan, H. Li, W. Zhang, L. Lv and J. Wu, Selective removal of Cu(II) ions by using cation-exchange resin-supported polyethyleneimine (PEI) nanoclusters, *Environ. Sci. Technol.*, 2010, **44**(9), 3508–3513.
17 W. Kong, Y. Liu and F. Liu, Scalable preparation of micro-meso-macroporous polymeric solid acids spheres from controllable sulfonation of commercial XAD-4 resin, *Ind. Eng. Chem. Res.*, 2018, **57**(42), 14080–14087.
18 L. L. Wang, C. Ling, B. S. Li, D. S. Zhang, C. Li, X. P. Zhang and Z. F. Shi, Highly efficient removal of Cu(II) by novel dendritic polyamine-pyridine-grafted chitosan beads from complicated salty and acidic wastewaters, *RSC Adv.*, 2020, **10**(34), 19943–19951.
19 A. Baraka, P. J. Hall and M. J. Heslop, Melamine-formaldehyde-NTA chelating gel resin: Synthesis, characterization and application for copper(II) ion removal from synthetic wastewater, *J. Hazard. Mater.*, 2007, **140**(1–2), 86–94.
20 J. Jiang, X.-S. Ma, L.-Y. Xu, L.-H. Wang, G.-Y. Liu, Q.-F. Xu, J.-M. Lu and Y. Zhang, Applications of chelating resin for heavy metal removal from wastewater, *e-Polymers*, 2015, **15**(3), 161–167.
21 L. Zhang, A. Li, J. Wang, Y. Lu and Y. Zhou, A novel aminated polymeric adsorbent for removing refractory dissolved organic matter from landfill leachate treatment plant, *J. Environ. Sci.*, 2009, **21**(8), 1089–1095.
22 H. Wang, Z. Wang, R. Yue, F. Gao, R. Ren, J. Wei, X. Wang and Z. Kong, Rapid preparation of adsorbent based on mussel inspired chemistry and simultaneous removal of heavy metal ions in water, *Chem. Eng. J.*, 2020, **383**, 123107.
23 C. Liu, R. Bai, L. Hong and T. Liu, Functionalization of adsorbent with different aliphatic polyamines for heavy metal ion removal: Characteristics and performance, *J. Colloid Interface Sci.*, 2010, **345**(2), 454–460.
24 J. H. Sherman, N. D. Danielson, R. T. Taylor, J. R. Marsh and D. T. Esterline, Removal of transition metals from motor oil using ion exchange resins, *Environ. Technol.*, 1993, **14**(11), 1097–1100.
25 M. Pan, S. Liu and J. W. Chew, Realizing the intrinsic electrochemical activity of acidic N-doped graphene through 1-pyrenesulfonic acid bridges, *Adv. Funct. Mater.*, 2020, 2001237.
26 Y. Zhang, C. Zhu, F. Liu, Y. Yuan, H. Wu and A. Li, Effects of ionic strength on removal of toxic pollutants from aqueous media with multifarious adsorbents: A review, *Sci. Total Environ.*, 2019, **646**, 265–279.
27 M. Song and M. Li, Adsorption and regeneration characteristics of phosphorus from sludge dewatering filtrate by magnetic anion exchange resin, *Environ. Sci. Pollut. Res.*, 2019, **26**(33), 34233–34247.
28 M. Monier and D. A. Abdel-Latif, Preparation of cross-linked magnetic chitosan–phenylthiourea resin for adsorption of Hg(II), Cd(II) and Zn(II) ions from aqueous solutions, *J. Hazard. Mater.*, 2012, **209–210**, 240–249.
29 J. Fu, J. Zhu, Z. Wang, Y. Wang, S. Wang, R. Yan and Q. Xu, Highly-efficient and selective adsorption of anionic dyes onto hollow polymer microcapsules having a high surface-density of amino groups: Isotherms, kinetics, thermodynamics and mechanism, *J. Colloid Interface Sci.*, 2019, **542**, 123–135.
30 L. Xu, Y. Liu, J. Wang, Y. Tang and Z. Zhang, Selective adsorption of Pb(2+) and Cu(2+) on amino-modified attapulgite: Kinetic, thermal dynamic and DFT studies, *J. Hazard. Mater.*, 2021, **404**(Pt A), 124140.
31 M. Pan, J. Ding, L. Duan and G. Gao, Sunlight-driven photo-transformation of bisphenol A by Fe(III) in aqueous solution: Photochemical activity and mechanistic aspects, *Chemosphere*, 2017, **167**, 353–359.
32 M. A. Brown, A. Goel and Z. Abbas, Effect of electrolyte concentration on the stern layer thickness at a charged interface, *Angew. Chem., Int. Ed.*, 2016, **55**(11), 3790–3794.
33 F. Ahmadijokani, S. Tajahmadi, A. Bahi, H. Molavi, M. Rezakazemi, F. Ko, T. M. Aminabhavi and M. Arjmand, Ethylenediamine-functionalized Zr-based MOF for efficient removal of heavy metal ions from water, *Chemosphere*, 2021, **264**(Pt 2), 128466.
34 R. R. Navarro, K. Tatsumi, K. Sumi and M. Matsumura, Role of anions on heavy metal sorption of a cellulose modified with poly(glycidyl methacrylate) and polyethyleneimine, *Water Res.*, 2001, **35**(11), 2724–2730.
35 C. Zhu, F. Liu, C. Xu, J. Gao, D. Chen and A. Li, Enhanced removal of Cu(II) and Ni(II) from saline solution by novel dual-primary-amine chelating resin based on anion-synergism, *J. Hazard. Mater.*, 2015, **287**, 234–242.
36 A. Dehghan Monfared, M. H. Ghazanfari, M. Jamialahmadi and A. Helalizadeh, Adsorption of silica nanoparticles onto calcite: Equilibrium, kinetic, thermodynamic and DLVO analysis, *Chem. Eng. J.*, 2015, **281**, 334–344.
37 A. M. Smith, P. Maroni and M. Borkovec, Attractive non-DLVO forces induced by adsorption of monovalent organic ions, *Phys. Chem. Chem. Phys.*, 2017, **20**(1), 158–164.
38 D. Gentili and G. Ori, Reversible assembly of nanoparticles: theory, strategies and computational simulations, *Nanoscale*, 2022, **14**, 14385.